

Microwave Interferometry Based On Open-ended Coaxial Technique for High Sensitivity Liquid Sensing

Hind Bakli^{1,2*} and Kamel Haddadi²

¹Department of Sciences and Technologies, Tipaza, Algeria

²Institute of Electronics, Microelectronics and Nanotechnology, University Lille 1, Villeneuve d'Ascq, France

*corresponding authors, E-mail: baklih@yahoo.com, kamel.haddadi@iemn.univ-lille1.fr

Abstract

This paper describes a modified open-ended coaxial technique for microwave dielectric characterization in liquid media. A calibration model is developed to relate the measured transmission coefficient to the local properties of the sample under test. As a demonstration, the permittivity of different sodium chloride solutions is experimentally determined. Accuracies of 0.17% and 0.19% are obtained respectively for the real and imaginary parts of dielectric permittivity at 5.9 GHz.

1. Introduction

As a versatile tool for measuring the real and imaginary parts of the complex permittivity of dielectric materials, the open-ended coaxial probe has found widespread use in biomedical and food applications [1]. Advantages of the open-ended coaxial such as broadband frequency coverage and no sample preparation make the method a good candidate for liquid and semisolid samples [2]-[3]. However, in contrast with resonant methods, the technique suffers from a lack of sensitivity and accuracy for the determination of slight dielectric contrasts.

In this work, a novel approach based on the combination of the coaxial line method and an interferometric technique is proposed for the electromagnetic characterization of materials. In Section 2, we present the measuring principle based on the association of a coaxial probe and an interferometric set-up. In section 3, instrumentation for the dielectric characterization of liquid based on the interferometric technique is developed. An experimental study related to the detection and evaluation of small concentrations of sodium chloride in aqueous medium shows that the proposed technique is at the state of art in terms of operating frequency range, sensitivity and measurement accuracy. In section 4, a quasi-static approach is used to model the open-ended aperture admittance when a dielectric medium is set to the probe contact. Finally, in section 5, a calibration model is developed to relate the measured transmission coefficient to the local properties of the sample under test. As a demonstration, the permittivity

of different sodium chloride (NaCl) aqueous solutions is experimentally extracted.

2. Interferometric technique

2.1. Problematic of high impedances measurement

This paragraph highlights the problematic of the microwave measurement, based on a conventional vector network analyzer (VNA), of high impedances. The main measurement limitation relies in the impedance mismatch between the intrinsic impedance of the network analyzer close to 50 Ω and the high impedance of the device under test (DUT). The reflection coefficient measured by the VNA is expressed as

$$\Gamma = \frac{Z - Z_0}{Z + Z_0} \quad (1)$$

Where Z_0 is the 50 Ω reference impedance of the VNA. The situation is illustrated in Fig. 1 which represents the reflection coefficient Γ as a function of a real impedance.

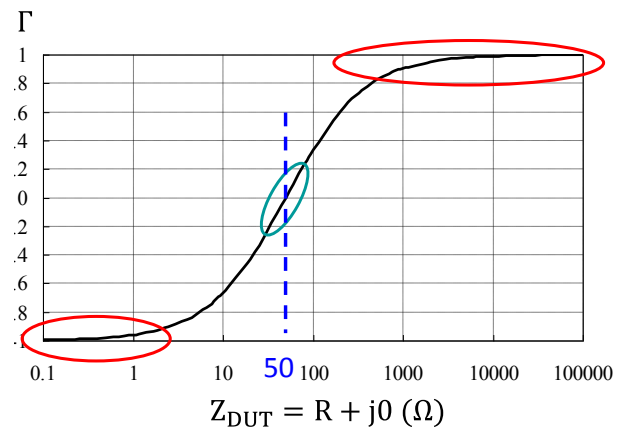


Figure 1: Reflection coefficient Γ as a function of a real impedance Z_{DUT} .

One can note that the measurement sensitivity is maximum for impedances around 50 Ω. But when very high impedances (or very low) are considered, the VNA becomes practically insensitive to the variations of the reflection

coefficient.

Consequently, there is an urgent need to extend the VNA measurement capabilities for impedances greater than the $k\Omega$.

2.2. Principle of the interferometric technique

The proposed interferometric technique consists to cancel the wave reflected by a high impedance device by combining it to a second one called ‘cancellation wave’. The reflected and the cancellation waves have the same magnitude but are phase-shifted by 180° . Consequently, the total reflected signal is theoretically zero. In other words, this technique brings the high impedance to 50Ω .

Ideally, the cancellation technique should be done under any configurations in terms of operating frequency, impedance, and level of the magnitude of the reflection coefficient. To that end, a measurement set-up is proposed in Fig. 2. This later is built up with a VNA, two power dividers, an impedance tuner (variable attenuator connected to a phase-shifter) and an amplifier.

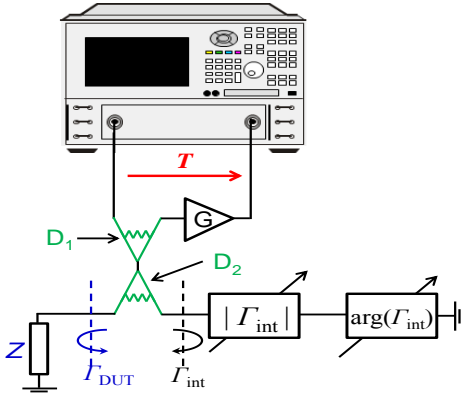


Figure 2: High impedance measurement system configuration based on interferometry.

In this configuration, the microwave signal is delivered from the port 1 of the VNA to feed the input of the first power divider D_1 . At the output of D_1 , the signal is divided between the two ports of the second power divider to supply the device under test (DUT) and the impedance tuner with reflection coefficients respectively Γ_{DUT} and Γ_{INT} . The reflected signals cross again D_1 and D_2 before being amplified (gain G) and then injected on port 2 of the VNA. The measured transmission coefficient T considering ideal components is given by

$$T = \frac{G}{4} (\Gamma_{DUT} + \Gamma_{INT}), \quad (2)$$

The main advantages of this configuration are: (i) the measurement is done in a transmission mode to overcome the main limitation of measurement accuracy encountered when using VNA's in terms of directivity errors, especially for the measurement of small signals. (ii) This architecture provides the possibility to insert an amplifier to further enhance the measurement sensitivity and accuracy.

Before performing a measurement, the interferometric system must be set to a frequency of operation and a given reference device Z_{REF} (reflection coefficient Γ_{REF}) connected to the measurement port (in place of Z_{DUT}). The reflection coefficient Γ_{INT} is then adjusted by the impedance tuner to cancel the reflection coefficient Γ_{REF} at the frequency of interest. Thus, the impedance tuner generates a wave with same magnitude and phase-shifted by 180° in comparison with the wave reflected by the reference impedance. In this condition, the transmission coefficient measured by the network analyzer is therefore zero.

After this step, the device under test is connected to the measurement port. The reflection coefficient of the device is retrieved from the measured transmission coefficient T by inverting the equation (2).

$$\Gamma_{DUT} = \frac{4T}{G} - \Gamma_{REF} \quad (3)$$

The proposed method is suitable for a wide range of applications requiring the detection and measurement of low impedance contrasts. Based on this technique, authors have developed near field microscopy platforms for local dielectric characterization [4]-[7]. In this paper, we investigate the dielectric characterization in a liquid medium using an open-ended coaxial line sensor.

3. Experimental validation

3.1. Theoretical analysis

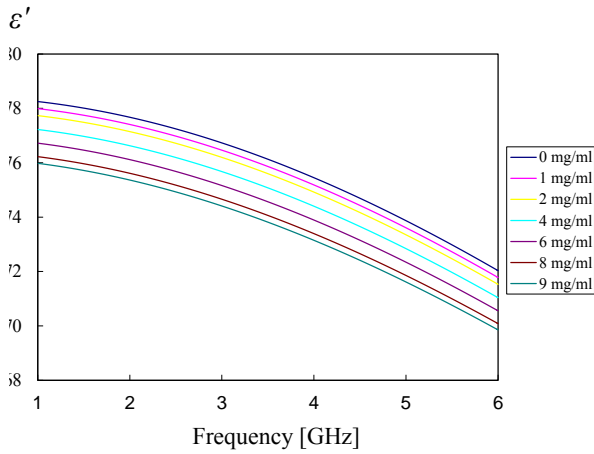
For the demonstration, we have investigated NaCl concentrations in solutions of de-ionized water at different test frequencies. The choice of NaCl solutions is motivated by the fact that it is the most abundant ionic fluid in biological samples. Therefore, sensitive detection of NaCl concentration may become a useful tool for studying the local electrical properties of samples. To remove parasitic capacitances between the probe and the liquid surface and to increase the probe-to-liquid electromagnetic coupling, the probe was immersed in the liquid at a $100 \mu\text{m}$ -depth. The complex permittivity of the aqueous solutions at 25°C as a function of the NaCl concentration are expressed from the following Cole–Cole model

$$\varepsilon = \varepsilon' - j\varepsilon'' + \frac{\sigma_i}{j\omega\varepsilon_0} = \varepsilon_\infty + \frac{\varepsilon_s - \varepsilon_\infty}{1 - (j\omega\tau)^{1-\alpha}} + \frac{\sigma_i}{j\omega\varepsilon_0} \quad (4)$$

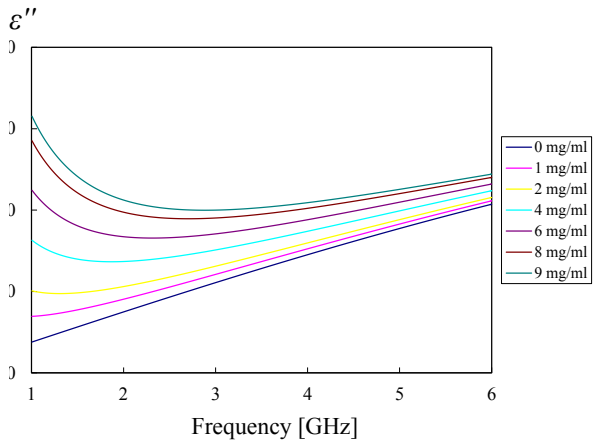
where ε_s and ε_∞ are the limit of the permittivity at low and high frequencies, τ is the relaxation time, σ_i is the ionic conductivity, ε_0 is the permittivity of free space and α is a distribution parameter. The parameters are calculated from empirical relationships derived from the literature [8]. From equation (4), we have determined the real and imaginary part of the complex permittivity for different NaCl solutions for small concentrations (less than 10 mg/ml) in the frequency band 1-6 GHz.

From figure 3 we note, when the NaCl concentration increases, a slight decrease of the value of the dielectric constant ε' in the frequency band considered. The variation of the NaCl in the solutions impacts a lot the dielectric

losses. In particular, a strong increase in the value of the imaginary part ϵ'' of the permittivity is observed for the lowest frequencies. The variation is mainly imputed to the increase of the ionic conductivity that is proportional to the NaCl concentration.



(a)



(b)

Figure 3: Frequency dependence of the complex permittivity for different NaCl solutions. (a) Real part of ϵ as a function of frequency. (b) Imaginary part of ϵ as a function of frequency.

3.2. Experimental validation

The proposed method is based on the test bench given in Fig. 4. The system consists of a network analyzer (Rhode & Schwarz ZVL6), two power dividers (Pasternack PE2028), an impedance tuner built up with a broadband variable attenuator with micrometric adjustments (Radiall R419133) and a high-resolution programmable delay line (Colby Instruments PDL-200A Series), a low noise amplifier and a coaxial probe. The container that holds the liquid sample is set on a xyz stage that offers a positioning accuracy of about ± 100 nm whereas the microwave parts of the microscope remains fixed during measurement. To complete the test bench, a data processing unit is used to control the position of the sample, to tune and record the transmission coefficient T measured by the VNA. The power of the microwave signal is set to -20 dBm and the intermediate

frequency bandwidth (IFBW) of the network analyzer to 10 Hz.

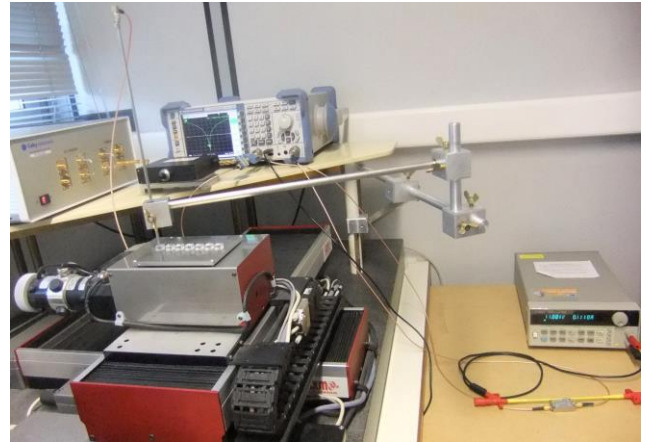
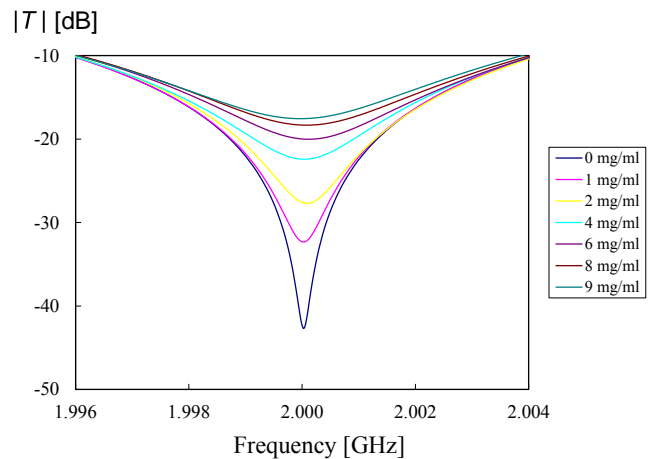


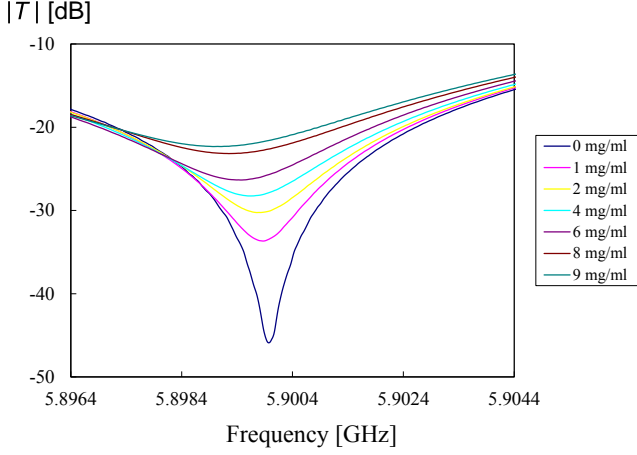
Figure 4: Experimental set-up based on interferometry.

The interferometric method has been tested for different frequencies in the range 2-6 GHz. We present in figure 5, the measured transmission coefficient magnitude for the different NaCl concentrations at the test frequency of 2 and 5.9 GHz. In this condition, the interferometry procedure is performed for a reference liquid corresponding to de-ionized water at an ambient temperature of 25°C. The quality factor at -3 dB bandwidth is set around 10000 and 21500 at 2 and 5.9 GHz respectively.

From this graphs, we can note that, when the NaCl concentration increases, the resonant frequency is shifted and the quality factor falls.



(a)



(b)

Figure 5: Measured transmission coefficient magnitude T for different NaCl concentrations: (a) at test frequency of 2 GHz, (b) at test frequency of 5.9 GHz.

4. Modeling of the open-ended coaxial probe

The open-ended aperture admittance can be expressed as [9]:

$$Y(\varepsilon_r) = j \frac{k^2}{\pi k_c \ln(b/a)} \int_a^b \int_a^b \int_0^\pi \cos\varphi \frac{e^{-jkr}}{r} d\varphi d\rho' d\rho, \quad (5)$$

where $k = \omega\sqrt{\varepsilon_r \varepsilon_0 \mu_0}$ is the wave vector in the medium, (ρ, ρ', φ) are the cylindrical coordinates, $r = \sqrt{\rho^2 + \rho'^2 - 2\rho\rho' \cos(\varphi)}$, and a et b are respectively the inner and outer radius of the probe (Table 1). $k_c = \omega\sqrt{\varepsilon_c \varepsilon_0 \mu_0}$ is the wave vector in the probe with ε_c set to 1.7.

When considering the quasi-static approach [9]-[10], equation (5) can be reduced to

$$Y(\varepsilon_r) = \frac{j2\omega\varepsilon_r}{(\ln(b/a))^2} \left(I_1 - \frac{k^2 I_3}{2} \right), \quad (6)$$

where

$$I_1 = \int_a^b \int_a^b \int_0^\pi \frac{\cos\varphi}{r} d\varphi d\rho' d\rho, \quad (7)$$

and

$$I_3 = \int_a^b \int_a^b \int_0^\pi r \cos\varphi d\varphi d\rho' d\rho, \quad (8)$$

I_1 and I_3 are independent of the medium characteristics, a quadratic equation in ε_r can be formulated using (6) for a measured admittance $Y(\varepsilon_r)$, which can be solved easily for ε_r .

$$I_3 \omega^3 \mu_0 j \varepsilon_r^2 - 2j\omega I_1 \varepsilon_r + Y(\varepsilon_r) (\ln(b/a))^2 = 0. \quad (9)$$

I_1 and I_3 are dependent only on the probe geometry. For the probe used, the calculated values of I_1 and I_3 are given in Table 1.

Table 1: Integrals I_1 and I_3 for the coaxial probe used.

a [mm]	b [mm]	I_1	I_3
0.535	1.458	0.01498	$-1.02994 \cdot 10^{-6}$

5. Calibration model and inverse problem

A traditional one port calibration model is used to make the link between the measured transmission coefficient T and the reflection coefficient at the end of the coaxial probe Γ_t . The resulting model is given by

$$T = E_{11} + \frac{E_{12}E_{21}\Gamma_t}{1 - E_{22}\Gamma_t}, \quad (10)$$

where the complex terms E_{11} , $E_{12}E_{21}$ and E_{22} are calibration coefficients that correspond respectively to the directivity, source match and reflection tracking errors. Three different NaCl solutions are used to determine these calibration coefficients. Thus, by measuring Γ_t , it is possible to determine Y and then retrieve the material permittivity ε_r . To determine the dielectric properties of the different NaCl solutions, the following steps are followed:

1- Estimation of the admittance of the three NaCl solutions (0, 4 and 9 mg/ml) selected for calibration (i.e. Y_{t1} , Y_{t2} , Y_{t3}) by using equation (6).

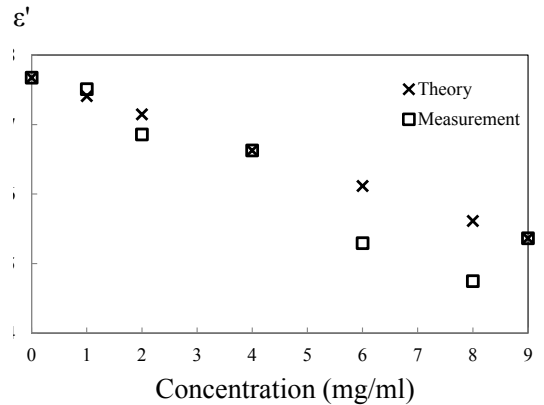
2- Determination of the reflection coefficients Γ_{t1} , Γ_{t2} and Γ_{t3} of the three known admittances Y_{t1} , Y_{t2} and Y_{t3} ($\Gamma_t = \frac{Y(\varepsilon_r) - Y_0}{Y(\varepsilon_r) + Y_0}$, $Y_0 = 50\Omega$).

3- Solving of the system (10) to find E_{11} , $E_{12}E_{21}$ and E_{22} .

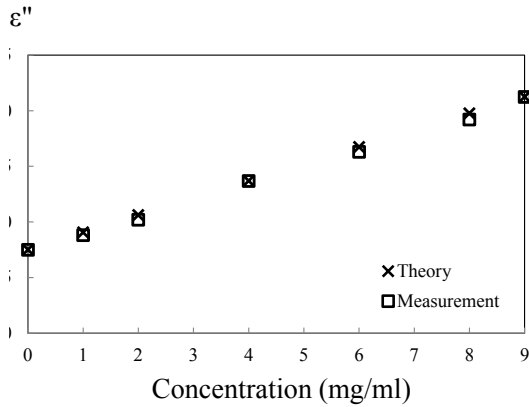
4- Determination of the reflection coefficient Γ_t for the remaining concentrations from the inversion of equation (10) and then calculation of Y .

5- Retrieval of the dielectric properties by the resolution of equation (9).

We present in figure 6 the dielectric permittivity reported from theory and determined experimentally for the different NaCl aqueous solutions considered at the test frequency of 2 GHz.



(a)

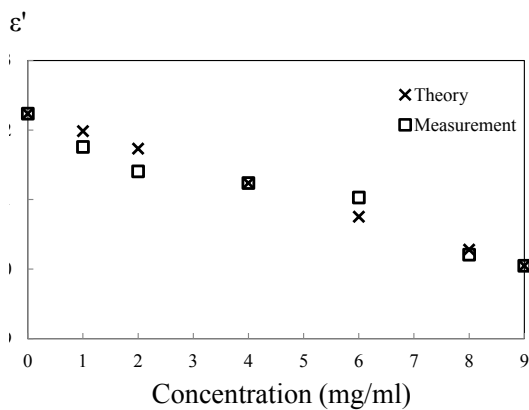


(b)

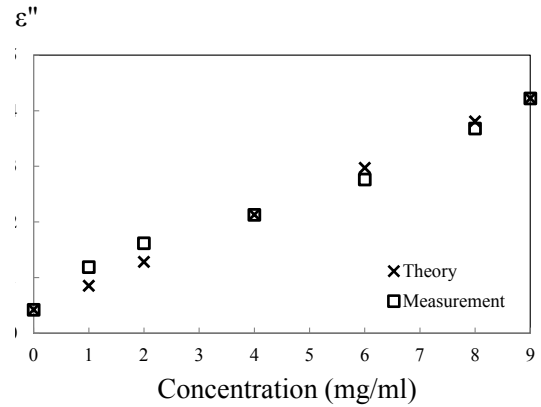
Figure 6: Theoretical and measured values of the dielectric permittivity for different NaCl aqueous solutions at 2 GHz: (a) real part ϵ' , (b) imaginary part ϵ'' .

From this graph, we can observe a good agreement between measurement and theory. The average accuracy at the test frequency of 2 GHz is found to be 0.4% and 0.3% on the real and imaginary parts of permittivity.

We present in figure 7 the dielectric permittivity reported from theory and determined experimentally for the different NaCl aqueous solutions considered at the test frequency of 5.9 GHz. From this graph, we can observe a good agreement between measurement and theory. The average accuracy at the test frequency of 5.9 GHz is found to be 0.17% and 0.19% on the real and imaginary parts of permittivity.



(a)



(b)

Figure 7: Theoretical and measured values of the dielectric permittivity for different NaCl aqueous solutions at 5.9 GHz: (a) real part ϵ' , (b) imaginary part ϵ'' .

6. Conclusion

A microwave interferometry based on open-ended coaxial technique was developed for high sensitivity liquid sensing applications. A calibration model was proposed to relate the measured transmission coefficient to the local properties of the liquid. The complex permittivity for different NaCl solutions was experimentally determined using the technique proposed at 2 and 5.9 GHz. Average accuracy of 0.17% and 0.19% were obtained respectively for the real and imaginary parts of the permittivity at the test frequency of 5.9 GHz.

References

- [1] T. H. Kim, J. K. Pack, Measurement of electrical characteristics of female breast tissues for the development of the breast cancer detector, *Progress In Electromagnetics Research C* 12: 188–199, 2012.
- [2] D. Popovic, L. McCartney, C. Beasley, M. Lazebnik, M. Okoniewski, S. C. Hagness, J. H. Booske, Precision open-ended coaxial probes for in vivo and ex vivo dielectric spectroscopy of biological tissues at microwave frequencies, *IEEE Trans. Microwave Theory and Techniques* 53: 1713-1722, 2005.
- [3] Agilent Technologies, Inc., Agilent 85070E Dielectric Probe Kit, 200 MHz to 50 GHz, <http://cp.literature.agilent.com/litweb/pdf/5989-0222EN.pdf>.
- [4] K. Haddadi, H. Bakli, T. Lasri, Microwave liquid sensing based on interferometry, *IEEE Microw. Wireless Components Letters* 22: 542–544, 2012.
- [5] H. Bakli, K. Haddadi, T. Lasri, Interferometric technique for scanning near-field microwave microscopy applications, *Proc. IEEE Instrum. Meas. Technol. Conference*, Minneapolis, USA, pp. 1694-1698, 2013.
- [6] H. Bakli, K. Haddadi, T. Lasri, Interferometric technique for scanning near-field microwave

- microscopy applications, *IEEE Trans. Instrumentation Measurement* 63: 1281–1286, 2014.
- [7] H. Bakli, K. Haddadi, T. Lasri, Modeling and calibration in near-field microwave microscopy for dielectric constant and loss tangent measurement, *IEEE Sensors Journal* PP: 1–2, 2016.
- [8] A. Peyman, C. Gabriel, E. H. Grant, Complex permittivity of sodium chloride solutions at microwave frequencies, *Bioelectromagnetics* 28: 264–274, 2007.
- [9] D. K. Misra, Quasi-Static Analysis of Open-Ended Coaxial Lines, *IEEE Trans. Microwave Theory and Techniques* 35: 925–928, 1987.
- [10] B. Filali, F. Boone, J. Rhazi, G. Ballivy, Design and calibration of a large open-ended coaxial probe for the measurement of the dielectric properties of concrete, *IEEE Trans. Microwave Theory and Techniques* 56: 2322–2328, 2008.